Equation of state and phase transitions in asymmetric nuclear matter

V. M. Kolomietz,[1] A. I. Sanzhur,[1,2] S. Shlomo,[2] and S. A. Firin[1]

[1]*Institute for Nuclear Research, Kiev 03680, Ukraine*

[2]*Cyclotron Institute, Texas A&M University, College Station, Texas 77843*

The structure of the three-dimension pressure-temperature-asymmetry surface of equilibrium of the asymmetric nuclear matter is studied within the thermal Thomas-Fermi approximation. Special attention is paid to the difference of the asymmetry parameter between the boiling sheet and that of the condensation sheet of the surface of equilibrium. We derive the condition of existence of the regime of retrograde condensation at the boiling of the asymmetric nuclear matter. We have performed calculations of the caloric curves in the case of isobaric heating. We have shown the presence of the plateau region in caloric curves at the isobaric heating of the asymmetric nuclear matter. The shape of the caloric curve depends on the pressure and is sensitive to the value of the asymmetry parameter. We point out that the experimental value of the plateau temperature $T \approx 7$ MeV corresponds to the pressure $P = 10^{-2}$ MeV/fm^3 at the isobaric boiling.

I. INTRODUCTION

At zero temperature, $T = 0$, a saturated nuclear matter is stable at vanishing pressure $P = 0$. As the temperature increases, the equilibrium state is derived through the isotherm (equation of state) $P(\rho, T)$, where ρ is the particle density. In general, there are two different regimes of the equilibrium state, see Ref. [1], Chap. 9. If the evaporation time is large enough and the evaporated particles are carried away from the heated liquid, the equilibrium condition is given by $P(\rho, T) = 0$, i.e., it has the same form as at $T = 0$. By increasing the temperature one can reach the so-called phase separation temperature T_s [2–4] above which the equilibrium condition $P(\rho, T) = 0$ is not satisfied anymore. This happens if the minimum of the isotherm $P(\rho, T)$ is shifted on the ρ axis and it is located at $\rho = \rho_{min} \neq 0$. The temperature T_s is then the limiting one for the existence of a stable state of the liquid phase under the equilibrium condition $P(\rho, T) = 0$. In another regime, the heated liquid is surrounded by the saturated vapor. The equilibrium condition requires then that the pressure, $P^{liq}(\rho, T)$, and the chemical potential, $\mu^{liq}(\rho, T)$, of the liquid phase should be equal to the corresponding ones, $P^{vap}(\rho, T)$ and $\mu^{vap}(\rho, T)$, for the saturated vapor, see Ref. [1], Chap. 8. (Here and below indices ''liq'' and ''vap'' denote the liquid and vapor phases, respectively.) In this regime, as the temperature increases, the liquid becomes unstable with respect to the phase transition (boiling) and the corresponding boiling temperature is the limiting one for the heating of the nuclear liquid.

The limiting temperatures and the critical behavior of the symmetric nuclear matter have been intensively investigated using an effective interaction and finite temperature self-consistent mean-field theory [4–7]. The thermal properties of asymmetric nuclear matter have been considered in Refs. [2–4,8–13]. In general, the two-component liquid and its saturated vapor co-exist with different asymmetry parameter X because of the ρ dependence of the symmetry energy. The equilibrium state of the two phases of a two-component system is described by the three-dimension surface of equilibrium in variables P, T, and X, see Ref. [1], Chaps. 8 and 9.

The evaluation of the (P, T, X) surfaces of equilibrium and the analysis of the boiling regime for an asymmetric nuclear matter is a main goal of the present paper. We also study the properties of the caloric curve in the two regimes described above.

II. EQUATION OF STATE OF HOT NUCLEAR MATTER

We will follow the temperature dependent Thomas-Fermi approximation using the Skyrme-type force as the effective nucleon-nucleon interaction. The energy density, $\mathcal{E}$, and the entropy density, $\mathcal{S}$, are given by [14]

$$\mathcal{E} = T \sum_q \mathcal{A}_q^* J_{3/2}(\eta_q) + \frac{1}{2} t_0 [(1 + x_0/2)\rho^2$$

$$- (x_0 + 1/2)(\rho_n^2 + \rho_p^2)] + \frac{1}{12} t_3 \rho^\sigma [(1 + x_3/2)\rho^2$$

$$- (x_3 + 1/2)(\rho_n^2 + \rho_p^2)], \tag{1}$$

$$\mathcal{S} = \sum_q \left(\frac{5}{3} \mathcal{A}_q^* J_{3/2}(\eta_q) - \eta_q \rho_q \right), \tag{2}$$

where x_i, t_i, and σ are the Skyrme force (SkM) parameters, q is the isospin index ($q = n$ for neutron and $q = p$ for proton), ρ_q is the nucleon density, and $\rho = \rho_n + \rho_p$. The Fermi integral $J_\nu(\eta_q) = \int_0^\infty dz z^\nu / (1 + \exp(z - \eta_q))$ in Eqs. (1) and (2) depends on the fugacity η_q. The value of η_q can be found from the condition

$$\rho_q = \mathcal{A}_q^* J_{1/2}(\eta_q). \tag{3}$$

Here, $\mathcal{A}_q^* = (1/2\pi^2)(2m_q^* T/\hbar^2)^{3/2}$ and m_q^* is the effective nucleon mass derived by

$$\frac{\hbar^2}{2m_q^*} = \frac{\hbar^2}{2m} + \frac{1}{4}[t_1(1 + x_1/2) + t_2(1 + x_2/2)]\rho$$

$$+ \frac{1}{4}[t_2(x_2 + 1/2) - t_1(x_1 + 1/2)]\rho_q. \tag{4}$$

Using Eqs. (1) and (2) one can derive the free energy density $\mathcal{F}=\mathcal{E}-T\mathcal{S}$. Finally, one obtains the pressure P (equation of state) and the chemical potentials μ_q. Namely,

$$P=\rho^2\left(\frac{\partial}{\partial\rho}\frac{\mathcal{F}}{\rho}\right)_{T,X},$$

$$\mu_n=\left(\frac{\partial\mathcal{F}}{\partial\rho_n}\right)_{T,\rho_p}, \quad \mu_p=\left(\frac{\partial\mathcal{F}}{\partial\rho_p}\right)_{T,\rho_n}, \quad (5)$$

where the asymmetry parameter X is defined as $X=(\rho_n-\rho_p)/\rho$. A numerical calculation of the pressure P with the energy density $\mathcal{E}$ from Eq. (1) leads to the van der Waals–like isotherms $P=P(T,X,\rho)$, describing both the liquid and the vapor phases [6,8–10]. According to Gibbs's phase rule, the equilibrium states of the two-phase (liquid + vapor) and the two-component (neutrons+protons) system are located on the three-dimensional surface in the (P,T,X) space. To obtain the shape of the (P, T, X) surface of equilibrium one should use the Gibbs equilibrium conditions [1]:

$$P^{\text{liq}}(T,X,\rho)=P^{\text{vap}}(T,X,\rho),$$

$$\mu_q^{\text{liq}}(T,X,\rho)=\mu_q^{\text{vap}}(T,X,\rho). \quad (6)$$

We will imply that the nuclear matter is a bound system of nucleons assuming that the following additional condition $\mu_q^{\text{liq}}<0$ is also satisfied.

III. SURFACES OF EQUILIBRIUM

We have performed calculations of the surfaces of equilibrium in (P, T, X) space using the SkM force [14] with the parameters $t_0=-2645$ MeV fm^3, $t_1=385$ MeV fm^5, $t_2=-120$ MeV fm^5, $t_3=15\,595$ MeV fm$^{3+3\sigma}$, $x_0=0.09$, $x_1=x_2=x_3=0$, and $\sigma=1/6$, adopted for the ground state of nuclei. We point out that the use of the Skyrme force from the ground-state calculations is a quite reasonable approximation for our purposes. The effective interaction is modified only by a few percent in a wide temperature region from 0 to 20 MeV [15,16]. The numerical procedure we used starts from certain values of X^{liq}, T, and looks for ρ^{liq}, ρ^{vap}, and X^{vap} that satisfy the equilibrium conditions (6).

The section of the equilibrium surface calculated by our code is shown in Fig. 1. This figure represents the equilibrium states having $X>0$, i.e., states of the neutron-rich nuclear matter. We point out that there are two sheets of the surface of equilibrium. The upper sheet is the surface of boiling and the lower one is the surface of condensation. The interior space between the sheets is the phase separation region where the two phases coexist. The crossing points of both sheets with a straight line $P=$ const and $T=$ const, give the equilibrium asymmetry parameters X^{liq} and X^{vap} for liquid and vapor phases, respectively. In general the asymmetry parameters X^{liq} and X^{vap} are different. The vapor asymmetry X^{vap} exceeds the corresponding liquid one X^{liq} (at $X^{\text{liq}}>0$). This is a feature of the nuclear matter. The density dependence of the isospin symmetry energy [see Eq. (1)] provides
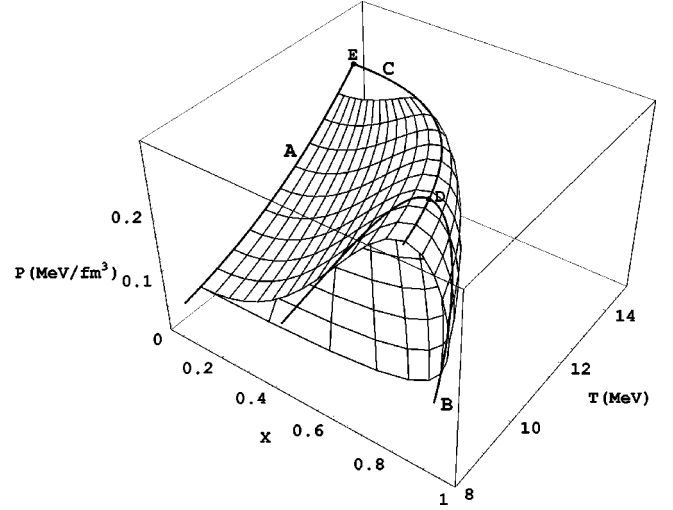

FIG. 1. Surface of equilibrium in (P,T,X) space. The upper sheet is the surface of boiling and the lower one is the surface of condensation. The azeotropic line and the critical line are marked by the letters A and C, respectively. The drip line $\mu_n=0$ is marked by the letter B. The point D indicates the maximum possible asymmetry for the bound liquid phase at $\mu_n<0$ and the point E is the critical point for the symmetric system $X=0$.

the condition $|\mu_n|<|\mu_p|$ and the preferable emission of neutrons.

The above mentioned sheets of the surface of equilibrium coincide along the azeotropic (P,T) line in $X=0$ plane denoted by letter A in Fig. 1. The azeotropic line is cut off at the critical temperature $T_{\text{cr}}^{(\text{sym})}=14.61$ MeV (point E) of the symmetric nuclear matter derived by the condition [1]

$$\left(\frac{\partial P}{\partial\rho}\right)_{T,X=0}=\left(\frac{\partial^2 P}{\partial\rho^2}\right)_{T,X=0}=0. \quad (7)$$

Both sheets of the surface of equilibrium also coincide along the critical line marked by letter C in Fig. 1. The critical line of an asymmetric nuclear matter is derived by the condition, see Ref. [1], Chap. 9,

$$\left(\frac{\partial\mu_q}{\partial X}\right)_{T,P}=\left(\frac{\partial^2\mu_q}{\partial X^2}\right)_{T,P}=0. \quad (8)$$

We point out that the critical temperature T_{cr} derived by Eq. (8) at $X\neq0$ is different from the one, $T_{\text{cr}}^{(\text{sym})}$, obtained from Eq. (7). If one goes along the critical line C, the critical temperature T_{cr} decreases and the corresponding pressure increases as the value of X increases.

The line B in Fig. 1 is the line with $\mu_n=0$. The crossing point of the critical line C with the line B (point D in Fig. 1) provides the maximum possible asymmetry for the bound ($\mu_q^{\text{liq}}<0$) liquid phase. This point is located at $X=0.68$, $T=10.4$ MeV, and $P=0.26$ MeV/fm^3 for the SkM interaction. Note that the cold nuclear matter at $T=0$ is bound at $X<0.31$. Thus, the hot nuclear matter can exist (in the bound state) at higher asymmetry than the cold one. This feature of
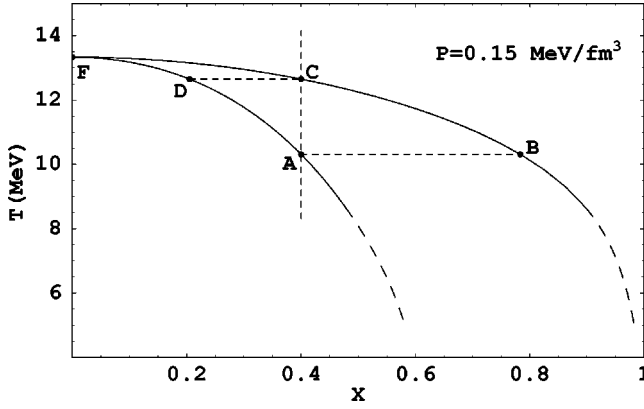
FIG. 2. A cut of the (P,T,X) surface of equilibrium by the plane $P=0.15$ MeV/fm$^3 < P_{cr}^{(sym)}$.

hot nuclear matter appears because of the increasing of the symmetry energy with temperature.

IV. BOILING AND CALORIC CURVES

Let us consider the isobaric (T,X) phase diagrams obtained as the cut of the equilibrium surface of Fig. 1 by plane $P=P_{ext}=$ const. These diagrams are very useful for obtaining an insight into the liquid-vapor phase transition in hot asymmetric nuclear matter. The shape of (T,X) diagram depends on the value of the pressure P_{ext}. The (T,X) diagram contains the critical point T_{cr} if the value of pressure P_{ext} exceeds the critical (maximal allowed) pressure $P_{cr}^{(sym)}$ on the azeotropic line in Fig. 1. For the SkM force used here, the value of the critical pressure obtained from Eq. (7) is $P_{cr}^{(sym)}=0.2109$ MeV/fm^3. In the opposite case $P_{ext} < P_{cr}^{(sym)}$, the (T,X) diagram contains the point of equal concentration $X=0$. In Figs. 2 and 3 we have plotted the (T,X) diagrams at the pressures $P_{ext}=0.15$ MeV/fm^3 and $P_{ext}=0.25$ MeV/fm^3, respectively. In each diagram we have two lines. The lower line (on the left) is the line of boiling and the upper line (on the right) is the line of condensation. In Fig. 2, these lines meet at the point of equal concentration $(X=0)$ and in Fig. 3, they meet at the critical point T_{cr}. The space between the boiling and condensation lines corresponds to the states of coexisting phases.
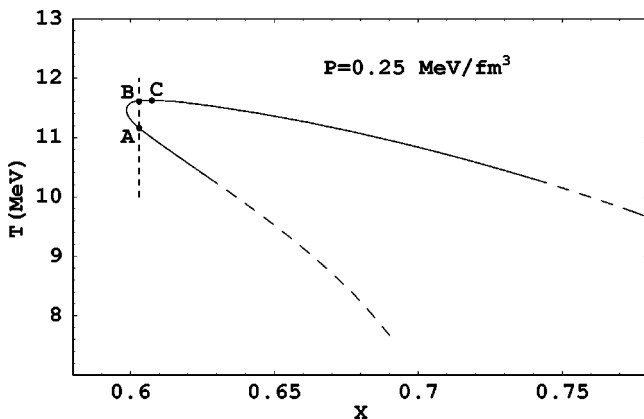

FIG. 3. The same as in Fig. 2 for $P=0.25$ MeV/fm$^3 > P_{cr}^{(sym)}$.

Let us consider the boiling of the asymmetric nuclear matter at the fixed external pressure $P_{ext} < P_{cr}^{(sym)}$, see Fig. 2. With the increase of temperature T at a certain asymmetry parameter $X=X_A^{liq}$, the asymmetric nuclear matter begins to boil at temperature T_A on the line of boiling (point A in Fig. 2). The boiling process is accompanied by the preferable evaporation of neutrons because of the condition $|\mu_n| < |\mu_p|$. The liquid phase is then shifted to a more symmetric state and the boiling temperature increases due to the evaporation of the less-bound particles. The final state of system depends on the regime of heating. In regime I we assume that the liquid is evaporated in a free space and the vapor is taken away, the system moves along the surface of equilibrium to the point F, i.e., reaches the symmetric state $X=X_F^{liq}=0$ at $T=T_{max} < T_{cr}^{(sym)}$ on the azeotropic line. The boiling is finished then at fixed $T=T_{max}$ and $X=0$. The asymmetry of the vapor, X^{vap}, decreases with increasing T and disappears at $T=T_{max}$. This means, for instance, that the yield of symmetric clusters at the condensation of the vapor phase has to grow with T. In regime II we assume that the vapor remains near the liquid (at fixed pressure $P=P_{ext}$, this means an evaporation into a closed but not a fixed volume), the system moves along the boiling line and reaches the point D in Fig. 2. The point D corresponds to a fully evaporated liquid at asymmetry X_C^{vap} of the vapor (point C on the surface of condensation) that equals to the starting asymmetry X_A^{liq} of the liquid phase. We point out that, in general, the trajectory of motion of the liquid phase along the surface of equilibrium can be located beyond the plane $P=$ const and Fig. 2 should be considered as a formal illustration of the behavior of the heating system for the regime II where both points A and D are taken at different pressures. An analogous analysis of the boiling of the asymmetric nuclear matter can also be done in the case of $P_{ext} > P_{cr}^{(sym)}$, see Fig. 3. However, the presence of the critical point on the (T,X) phase diagrams in Fig. 3 leads to a very specific effect of the retrograde condensation, see also Refs. [1,12]. If one goes along straight line AB in Fig. 3 (at closed volume), the liquid starts to boil at temperature T_A. An increase of the temperature leads to an increase of the evaporation. However, the evaporation begins to decrease at certain temperature $T < T_B$ and the vapor disappears at temperature $T_B < T_C$.

The (T,X) phase diagrams allow us to study the shape of the caloric curve for the case of isobaric heating. We will consider the case of the evaporation in a closed (but not fixed) volume at the fixed pressure $P < P_{cr}^{(sym)}$, i.e., regime II in Fig. 2. Let us introduce the volume fractions λ^{liq} and λ^{vap} of the liquid and vapor phases defined by $\lambda^{liq}=V^{liq}/V$ and $\lambda^{vap}=V^{vap}/V$, where V^{liq} and V^{vap} are the volumes of the liquid and vapor phases, respectively, and $V=V^{liq}+V^{vap}$. The excitation energy per particle, E^*/A, is given by

$$\frac{E^*}{A} = \frac{\lambda^{liq}\mathcal{E}^{liq}(\rho^{liq},X^{liq},T)+\lambda^{vap}\mathcal{E}^{vap}(\rho^{vap},X^{vap},T)}{\lambda^{liq}\rho^{liq}+\lambda^{vap}\rho^{vap}}$$

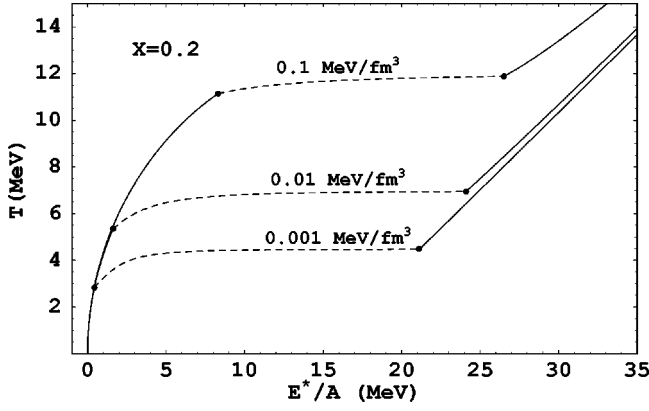$$-\left(\frac{\mathcal{E}^{liq}(\rho^{liq},X^{liq},T)}{\rho^{liq}}\right)_{T=0}, \qquad (9)$$

FIG. 4. Caloric curves for the isobaric heating of the asymmetric nuclear matter in regime II for different pressure P shown near the curves at fixed asymmetry parameter $X=0.2$.

where $\mathcal{E}^{\text{liq}}(\rho^{\text{liq}},X^{\text{liq}},T)$ and $\mathcal{E}^{\text{vap}}(\rho^{\text{vap}},X^{\text{vap}},T)$ are, respectively, the energy densities of the liquid and vapor phases, derived by Eq. (1) and taken at the corresponding values of the particle density ρ and the asymmetry parameter X. Let us consider a certain asymmetry parameter $X=X_0$. To calculate the excitation energy E^*/A we note that $\lambda^{\text{liq}}=1$, $\lambda^{\text{vap}}=0$, and $X^{\text{liq}}=X_0$ if T is below the boiling line and $\lambda^{\text{liq}}=0$, $\lambda^{\text{vap}}=1$, and $X^{\text{vap}}=X_0$ if T is above the condensation line in the (T,X) phase diagram of Fig. 2. In the case of coexisting phases (space between lines of the boiling and the condensation in Fig. 2) the required values of λ^{liq}, λ^{vap}, ρ^{liq}, ρ^{vap}, X^{liq}, and X^{vap} can be found using the following procedure. At given X_0, we go along the straight line $T=$const in both directions and get the cross points with the boiling and condensation lines that provide the asymmetry parameters X^{liq} and X^{vap} and the densities ρ^{liq} and ρ^{vap} for both phases. The volume fractions λ^{liq} and λ^{vap} are then determined by the following equations:

$$X_0=\frac{\lambda^{\text{liq}}\rho^{\text{liq}}X^{\text{liq}}+\lambda^{\text{vap}}\rho^{\text{vap}}X^{\text{vap}}}{\lambda^{\text{liq}}\rho^{\text{liq}}+\lambda^{\text{vap}}\rho^{\text{vap}}}, \quad \lambda^{\text{liq}}+\lambda^{\text{vap}}=1. \quad (10)$$

Caloric curves determined by Eq. (9) for $X=0.2$ and pressures $P=10^{-3}$ MeV/fm^3, 10^{-2} MeV/fm^3, and 10^{-1} MeV/fm^3 are presented in Fig. 4. The solid line at low values of the excitation energy E^*/A corresponds to the heating of the degenerate Fermi liquid with $E^*/A\sim T^2$. The solid line at high excitation energy E^*/A describes the classical Boltzmann's gas with $E^*/A=(3/2)T$. The region of two phase coexistence is displayed by the dashed line. The caloric curve is a continuous function of E^*/A and has a break in its derivative at two points connecting the two-phase region with the corresponding single-phase regions. As seen from Fig. 4, the plateau region corresponds to the two-phase region. A small increase of the dashed line with T is due to the motion along the boiling path AD in Fig. 2. The value of the plateau temperature increases with the increase of pressure. Experimental observations show a nearly flat caloric curve with a temperature of about 7 MeV [17]. If one could assume the process of isobaric heating for the description of the experimental data, the order of magnitude of the pressure
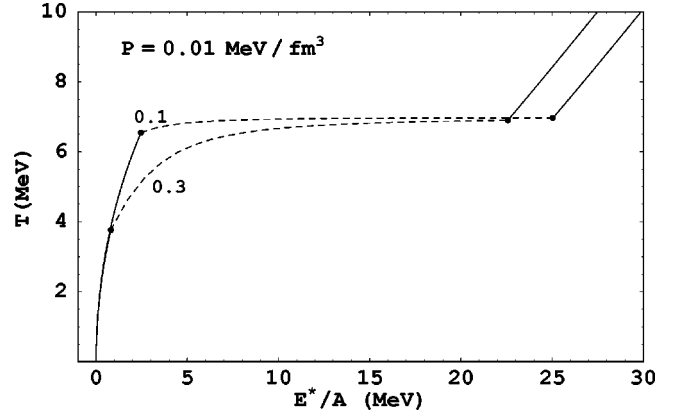
should be 10^{-2} MeV/fm^3 for this process. To obtain more accurate estimation an analysis of the contribution of both the surface and the Coulomb forces into the equilibrium condition (6) is needed [13,18].

The asymmetry dependence of the shape of the caloric curve is displayed in Fig. 5 by plotting two curves at $X=0.1$ and 0.3. The figure shows that the plateau temperature is slightly sensitive to the asymmetry parameter. At low asymmetry the two-phase region of the caloric curve is flatter and it is shifted to the higher values of E^*/A as compared to the case of high asymmetry.

Figure 6 shows results of the calculation of the caloric curve assuming the regime I, i.e., the case when vapor is taken away from the liquid during the boiling. The calculation was carried out for the values of pressure 10^{-3}, 10^{-2}, and 10^{-1} MeV/fm^3. The solid lines correspond to the heating of the liquid from $T=0$ to $T=T_A$ with asymmetry parameter $X=0.2$. The regions where saturated vapor is present (but taken away) are displayed by dashed lines. It is seen

FIG. 5. The same as in Fig. 4 for the fixed pressure $P=0.01$ MeV/fm^3 and different values of the asymmetry parameter X shown near the curves.
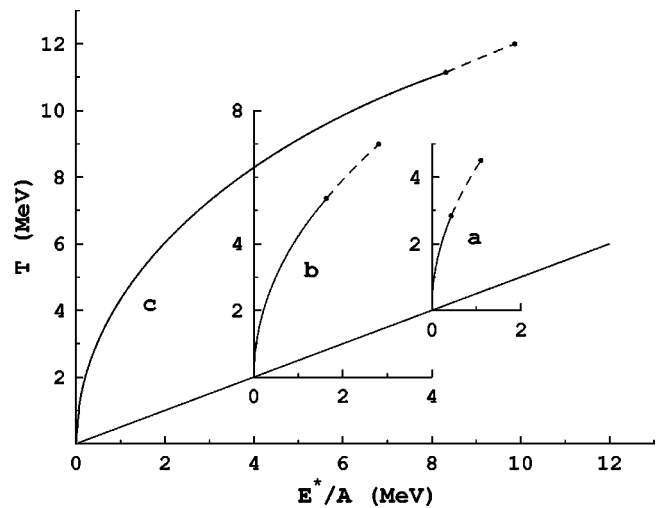

FIG. 6. Caloric curves for the isobaric heating in the case when vapor is being taken away from liquid (regime I). Calculations presented for values of pressure 10^{-3} MeV/fm^3 (a), 10^{-2} MeV/fm^3 (b), and 10^{-1} MeV/fm^3 (c).

from Fig. 6 that the value of the external pressure does not change the shape of the caloric curve calculated for regime I. Only the interval of E^*/A is sensitive to the value of the pressure.

V. SUMMARY

Starting from the temperature dependent Thomas-Fermi approximation with the effective SkM force, we have evaluated the three-dimensional (P,T,X) surface of equilibrium of the asymmetric nuclear matter. The (P,T,X) surface of equilibrium contains two sheets that correspond to the boiling and the condensation. Both sheets coincide along the azeotropic line and along the line of the critical pressure marked by C in Fig. 1. In general, the vapor asymmetry X^{vap} on the surface of condensation exceeds significantly the corresponding liquid asymmetry X^{liq} (at $X^{liq}>0$) lying on the surface of boiling. This is due to the fact that the isospin symmetry energy causes a preferable emission of neutrons. The surface of equilibrium is restricted by the drip line (line B in Fig. 1) where one has $\mu_n=0$. The (P,T,X) surface of equilibrium in Fig. 1 shows also that the hot nuclear matter exists (in a bound state) at higher asymmetry than the cold one due to the increase of the symmetry energy with temperature.

Our analysis of the isobaric (T,X) phase diagrams (see Figs. 2 and 3) shows that the process of isobaric boiling of the asymmetric nuclear matter depends on the value of the fixed pressure P_{ext}. In the case of enough low pressure $P_{ext}<P_{cr}^{(sym)}=0.2109$ MeV/fm^3 the (T,X) diagram contains the point of equal concentration $X=0$ and the process of boiling is accompanied by a decrease of the vapor asymmetry with increasing temperature T. In the case of high pres-

sure $P_{ext}>P_{cr}^{(sym)}$, the process of boiling leads to the very specific effect of a retrograde condensation with growing temperature T, see Fig. 3.

We have shown in Figs. 4 and 5 that the caloric curve for the process of isobaric heating of the asymmetric nuclear matter contains a plateau region where both the liquid and the saturated vapor phases co-exist. The position of the plateau region on the caloric curve depends on the pressure P_{ext} and is almost insensitive to a change in the asymmetry parameter X. As can be seen from Fig. 5, the shape of the caloric curve is significantly changed with asymmetry. At low asymmetry the two-phase region of the caloric curve is flatter. We pointed out that the experimental observation of the saturation of the caloric curve at temperature of about 7 MeV is obtained in our approach as an isobaric boiling of the nuclear liquid at the pressure $P_{ext}\approx10^{-2}$ MeV/fm^3. Note, however, that the effects of nuclear surface and Coulomb interaction are not included in our study. The asymmetry parameter X^{vap} of the vapor phase decreases along the boiling path of the caloric curve (dashed line in Figs. 4 and 5). Thus, the present model predicts an increase of the yield of the symmetric clusters at the condensation of the vapor phase with an increase of the excitation energy E^*/A in the plateau region of the caloric curve.

[1] L. D. Landau and E. M. Lifshitz, *Statistical Physics* (Pergamon, Oxford, 1958).

[2] M. Abd-Alla, S. Ramadan, and M. Y. M. Hassan, Phys. Rev. C **36**, 1565 (1987).

[3] D. Bandyopadhyay, J. N. De, S. K. Samaddar, and D. Sperber, Phys. Lett. B **218**, 391 (1989).

[4] D. Bandyopadhyay, C. Samanta, S. K. Samaddar, and J. N. De, Nucl. Phys. **A511**, 1 (1990).

[5] W. A. Küpper, G. Wegmann, and E. R. Hilf, Ann. Phys. **88**, 454 (1974).

[6] G. Sauer, H. Chandra, and U. Mosel, Nucl. Phys. **A264**, 221 (1976).

[7] H. Jaqaman, A. Z. Mekjian, and L. Zamick, Phys. Rev. C **27**, 2782 (1983).

[8] J. M. Lattimer and D. G. Ravenhall, Astrophys. J. **223**, 314 (1978).

[9] D. Q. Lamb, J. M. Lattimer, C. J. Pethick, and D. G. Ravenhall, Nucl. Phys. **A360**, 459 (1981).

[10] J. M. Lattimer, C. J. Pethick, D. G. Ravenhall, and D. Q. Lamb, Nucl. Phys. **A432**, 646 (1985).

[11] M. Barranco and J. R. Buchler, Phys. Rev. C **22**, 1729 (1980).

[12] H. Müller and B. D. Serot, Phys. Rev. C **52**, 2072 (1995).

[13] S. J. Lee and A. Z. Mekjian, Phys. Rev. C **63**, 044605 (2001).

[14] M. Brack, C. Guet, and H.-B. Håkansson, Phys. Rep. **123**, 275 (1985).

[15] A. Lejeune, P. Grange, M. Martzolff, and J. Cugnon, Nucl. Phys. **A453**, 189 (1986).

[16] J. Cugnon, A. Lejeune, M. Baldo, and U. Lombardo, Nucl. Phys. **A492**, 173 (1989).

[17] J. Cibor *et al.*, Phys. Lett. B **473**, 29 (2000).

[18] S. Levit and P. Bonche, Nucl. Phys. **A437**, 426 (1985).